ResearchGate

See discussions, stats, and author profiles for this publication at: https://www.researchgate.net/publication/255771660

A highly active homogeneous ICAR ATRP of methyl methacrylate using ppm levels of organocopper catalyst

ARTICLE · JUNE 2013

DOI: 10.1039/C3PY00309D

CITATIONS
12

READS
36

6 AUTHORS, INCLUDING:

Pan Xq
Soochow University (PRC)
42 PUBLICATIONS **456** CITATIONS

SEE PROFILE

Available from: Pan Xq
Retrieved on: 26 January 2016

Polymer Chemistry

RSC Publishing

PAPER

View Article Online
View Journal

A highly active homogeneous ICAR ATRP of methyl methacrylate using ppm levels of organocopper catalyst

Cite this: DOI: 10.1039/c3py00309d

Ting Guo, Lifen Zhang, Xiangqiang Pan, Xiaohong Li, Zhenping Cheng* and Xiulin Zhu*

A highly active homogeneous bulk initiators for continuous activator regeneration atom transfer radical polymerization (ICAR ATRP) of MMA using ppm levels of organocopper catalyst $Cu(SC(S)N(C_4H_9)_2)_2$ or $Cu(SeC(Se)N(C_4H_9)_2)_2$ was carried out successfully for the first time. For example, even though the catalyst concentration was decreased to 1.9 ppm, the polymerization with the molar ratio of $[MMA]_0 : [ATRP\ initiator]_0 : [Cu(SC(S)N(C_4H_9)_2)_2]_0 : [PMDETA]_0 : [AIBN]_0 = 500 : 1 : 0.0015 : 0.1 : 0.2$ could be carried out at 65 °C with 44.6% monomer conversion in 290 min; at the same time, the number average molecular weight of the resultant PMMA was close to its theoretical value with a narrow molecular weight distribution ($M_{n,GPC}$ = 24 500 g mol^{-1}, M_w/M_n = 1.36).

Received 5th March 2013
Accepted 17th April 2013

DOI: 10.1039/c3py00309d

www.rsc.org/polymers

Published on 19 April 2013 on http://pubs.rsc.org | doi:10.1039/C3PY00309D
Downloaded by Soochow University China on 13/05/2013 12:53:07.

Introduction

Atom transfer radical polymerization (ATRP) has been one of the most important living radical polymerization (LRP) techniques in polymer chemistry to obtain polymers with predetermined molecular weights, narrow molecular weight distributions, desired compositions and molecular architectures, as well as high chain end-functionalities.[1] However, the fact that the catalyst concentration required in conventional ATRP is often as high as 0.1 M in bulk monomer[2] has limited the industrial application of ATRP significantly.

Recently many environmentally friendly methods, like removing and recycling catalysts, have been rapidly developed. There have been several attempts to remove and recycle the catalyst efficiently by extraction, precipitation and immobilization, or by biphasic systems.[3] However, catalyst separation is usually not a facile process, as it either requires tedious additional post-treatment, or the polymerization is carried out in a heterogeneous catalysis system, which usually results in low catalyst activity. Therefore, methods which decrease the amount of catalyst used in ATRP systems are highly desired for the application of ATRP. The big breakthrough has been the development of several new ATRP methods by Matyjaszewski's group: activators regenerated by electron transfer (ARGET) ATRP,[4] initiators for continuous activator regeneration (ICAR) ATRP,[2b,5] and e-ATRP.[6] The activators in these systems, namely lower oxidation state transition metals, can continuously regenerate from the deactivators formed through radical–radical termination by a large excess of reducing agent, which makes it possible to conduct ATRP using a significantly lower concentration of catalyst and furthermore, makes it possible for ATRP to be employed on an industrial scale.

In a typical ICAR ATRP system, an alkyl halide is used as an initiator and a very small amount of higher oxidation state transition metal is used as a catalyst. A large excess of thermal radical initiator with respect to catalyst such as azobis(isobutyronitrile) (AIBN) is usually used, which can continuously generate the activators by *in situ* reduction with the deactivators. Since 2006 some excellent works on ICAR ATRP have been reported using inorganic transition metal catalysts such as $CuBr_2$, $CuCl_2$, $FeCl_3 \cdot 6H_2O$ and $FeBr_3$.[5,7] Other than inorganic transition metal catalysts, organocatalysts such as CuCCPh, CuSPh, CuSBu, $Mt\{SC(S)NR_2\}_n$ (Mt = Fe(III), Fe(II), Ru(III), Cu(II), Cu(I); R = ethyl, butyl or benzyl; n = 1, 2 or 3) are usually used in normal ATRP or reverse ATRP systems.[8] They are usually oil-soluble, which make it possible to conduct ATRP in homogeneous conditions without solvent. In addition, most of them have an ultraviolet light sensitive ω-$SC(S)NR_2$ (DC) group, which can function as an iniferter to allow chain extension under UV irradiation, or act as a pseudo-halogen to initiate the ATRP. Therefore, organocatalysts have many advantages over inorganic catalysts.

In addition, organocatalysts with DC groups usually have more reducing power, and the DC anion has a higher affinity for Cu complexes than halide anions (Br^- and Cl^-).[9] Therefore, in order to reduce the amount of catalyst, two organocopper catalysts, $Cu(SC(S)N(C_4H_9)_2)_2$ and $Cu(SeC(Se)N(C_4H_9)_2)_2$ were introduced in an ICAR ATRP system, and the polymerization of methyl methacrylate (MMA) could be conducted with as low as ppm concentrations of catalyst while maintaining the features

Jiangsu Key Laboratory of Advanced Functional Polymer Design and Application, Department of Polymer Science and Engineering, College of Chemistry, Chemical Engineering and Materials Science, Soochow University, Suzhou, 215123, China. E-mail: chengzhenping@suda.edu.cn; xlzhu@suda.edu.cn; Fax: +86-512-65882787; +86-512-65112796

Published on 19 April 2013 on http://pubs.rsc.org | doi:10.1039/C3PY00309D
Downloaded by Soochow University China on 13/05/2013 12:53:07.

of "living"/controlled radical polymerization of ATRP. For example, a monomer conversion of 44.6% could be obtained in 4.8 h while keeping $M_w/M_n = 1.36$ at the ratio of $[MMA]_0 : [Cu(SC(S)N(C_4H_9)_2)_2]_0 : [AIBN]_0 = 500 : 0.0015 : 0.2$ (1.9 ppm Cu catalyst). In addition, it is worth noting that when $Cu(SeC(Se)N(C_4H_9)_2)_2$ was used as the catalyst, selenium-ended polymers with potential applications in pharmacochemistry[10] could be obtained *via* this kind of ICAR ATRP system.

Experimental section

Materials

Methyl methacrylate (MMA) (>99%) was purchased from Shanghai Chemical Reagents Co. Ltd (Shanghai, China), which was removed from the inhibitor by passing through a neutral alumina column. *N*,*N*-Dibutyldithiocarbamate copper ($Cu(SC(S)N\text{-}(C_4H_9)_2)_2$) (95%) was purchased from Wuxi Chemical Factory (Jiangsu, China) and recrystallized twice from ethanol. *N*,*N*,*N*′,*N*″,*N*″′-Pentamethyl-diethylenetriamine (PMDETA) (98%, Jiangsu Liyang Jiangdian Chemical Factory, China) was dried with a 4 Å molecular sieve and distillated under vacuum. Azobis(isobutyronitrile) (AIBN) was obtained from Shanghai Chemical Reagents Co. and purified by recrystallizing twice from methanol. Ascorbic acid (AsAc), tin 2-ethylhexanoate ($Sn(EH)_2$), toluene (analytical reagent), tetrahydrofuran (THF) (analytical reagent) and all other chemicals were obtained from Shanghai Chemical Reagents Co. and used as received unless mentioned. The difunctional initiator 1,4-(2-bromo-2-methylpropionato)benzene ($BMPB_2$) and the catalyst *N*,*N*′-dibutyldiselenocarbamate copper, $Cu(SeC(Se)N(C_4H_9)_2)_2$ were synthesized according to the literature.[11]

Synthesis of 1,4-(2-bromo-2-methylpropionato)benzene ($BMPB_2$)

1,4-Dihydroxybenzene (5.51 g, 0.05 mol), triethylamine (23 mL, 0.165 mol), and THF (250 mL) were added to a 500 mL three-necked round-bottom flask. The solution was bubbled with argon and cooled in an ice bath under stirring at 0 °C. 2-Bromoisobutyryl bromide (14.9 mL, 0.12 mol) was added slowly to the mixture and the reaction mixture was allowed to react overnight under stirring at room temperature. After reaction, the side product triethylammonium bromide was removed by filtration and the solvent was removed from the reaction mixture by rotatory evaporation. The product was recovered as a yellow powder, which was recrystallized three times from methanol to give the white crystalline powder of $BMPB_2$: yield, 18.2 g (89.2%). ^1H NMR ($CDCl_3$, 400 MHz): $\delta = 7.18$ ppm (s, 4H), 2.07 ppm (s, 12H).

Synthesis of *N*,*N*′-dibutyldiselenocarbamate copper ($Cu(SeC(Se)N(C_4H_9)_2)_2$)

Carbon diselenide (0.34 g, 2 mmol) in *n*-hexane (10 mL) was added dropwise to a solution of dibutylamine (0.52 g, 4 mmol) in *n*-hexane (10 mL) under stirring at −10 °C; a yellow precipitate began to separate during the addition process. The precipitate was removed by filtration immediately and washed once with *n*-hexane. After that, it was dissolved in 20 mL of 0.5 M NaOH to give a light yellow solution. Then it was added to a copper sulphate solution (10.0 g in 50 mL of water) at room temperature, and the purplish-black floccus primary product was obtained after filtration, which was then washed with water. The pure product was obtained after extraction with chloroform in a Soxhlet apparatus. It was a purplish-black crystalline powder ($Cu(SeC(Se)N(C_4H_9)_2)_2$): yield, 0.8 g (85%). Ultraviolet absorption spectrum (chloroform): absorption bands at 325 nm and 293 nm.

General procedure for ICAR ATRP of MMA

A dry ampule was filled with $Cu(SC(S)N(C_4H_9)_2)_2$ or $Cu(SeC(Se)N(C_4H_9)_2)_2$, PMDETA, AIBN, $BMPB_2$ and MMA with a predetermined molar ratio, and vibrated until the mixture became a homogeneous solution. The mixture was thoroughly bubbled with argon for about 10 min to eliminate the dissolved oxygen, then the ampule was flame-sealed and transferred into an oil bath held at the desired temperature (65 °C) by a thermostat to polymerize under stirring. After the desired polymerization time, the ampule was cooled by immersing it in iced water. Afterwards, it was opened and the contents were dissolved in THF (~2 mL), then precipitated into a large amount of methanol (~250 mL). The polymer obtained by filtration was dried under vacuum until a constant weight. The monomer conversion was determined gravimetrically.

Chain extension of PMMA

A typical photo-initiated polymerization of St *via* the iniferter mechanism for the molar ratio of $[St]_0 : [PMMA]_0 = 200 : 1$ is as follows: the macroinitiator PMMA (345.2 mg, 14 800 g mol^{-1}), fresh St (0.5 mL) and toluene (1.0 mL) were placed in an ampule, mixed and stirred to form a homogeneous solution. The solution was thoroughly bubbled with argon for about 10 min to eliminate the dissolved oxygen, then the ampule was flame-sealed and the mixture was polymerized under 365 nm UV light irradiation (with a 300 W high-pressure mercury vapor lamp at a distance of 50 cm) at room temperature for 6 hours. The rest of the procedures for precipitating and drying are the same as those described above. The block copolymerization of PMMA-*b*-PS *via* the ATRP mechanism using PMMA as the macroinitiator and CuBr/PMDETA as the catalyst are similar to that described above except for the different amounts of the corresponding chemicals.

Characterization

The number-average molecular weight ($M_{n,GPC}$) and molecular weight distribution (M_w/M_n) values of the polymers were determined using a Waters 1515 gel permeation chromatograph (GPC) equipped with a refractive index detector (Waters 2414) using HR 1 (pore size: 100, 100–5000 Da), HR 2 (pore size: 500, 500–20 000 Da), and HR 4 (pore size 10 000, 50–100 000 Da) columns (7.8 mm × 300 mm, 5 μm beads size) with measurable molecular weights ranging from 10^2 to 5×10^5 g mol^{-1}. THF was used as the eluent at a flow rate of 1.0 mL min^{-1} and 39.3 °C. GPC samples were injected using a Waters 717 plus

 This journal is © The Royal Society of Chemistry 2013

Published on 19 April 2013 on http://pubs.rsc.org | doi:10.1039/C3PY00309D
Downloaded by Soochow University China on 13/05/2013 12:53:07.

autosampler and calibrated with poly(methyl methacrylate) standards purchased from Waters. The ^{1}H NMR spectra were recorded on an Inova 400 MHz nuclear magnetic resonance (NMR) instrument using $CDCl_3$ as the solvent and tetramethylsilane (TMS) as the internal standard at ambient temperature. The UV-vis spectra were recorded using a Hitachi U-3900 spectrophotometer at room temperature.

Results and discussion

Effect of reaction components on polymerization of MMA using $Cu(SC(S)N(C_4H_9)_2)_2$ as the catalyst

Firstly, to optimize the polymerization conditions, three cheap reducing agents (RAs) which are commonly used in ATRP systems were investigated with the ratio of $[MMA]_0 : [BMPB_2]_0 : [Cu(SC(S)N(C_4H_9)_2)_2]_0 : [PMDETA]_0 : [RA]_0 = 500 : 1 : 0.005$ (6.3 ppm) : 1 : 0.2 (0.4) in bulk at 65 °C, and the results are shown in Table 1. It can be seen that when AsAc is used as the reducing agent (entry 1 in Table 1), the polymerization rate is the fastest, however it is uncontrollable ($M_w/M_n = 1.68$); when $Sn(EH)_2$ is employed (entry 2 in Table 1), although the controllability over molecular weight and molecular weight distribution is improved, the polymerization rate is slow. By comparison to the reducing agents AsAc and $Sn(EH)_2$, AIBN is the optimal one, with good controllability and faster polymerization rate (entry 3 in Table 1) due to better solubility in the polymerization system. Table 2 shows the effects of ligand and alkyl halide initiator on the polymerization of MMA. It can be seen that if no ligand (entry 2 in Table 2) or no alkyl halide initiator (entry 3 in Table 2) was used in the polymerization system, the molecular weights are much larger than the corresponding theoretical ones and the molecular weight distributions are much broader than that of normal ICAR ATRP (entry 1 in Table 2). In other words, the ligand and alkyl halide are necessary components for a successful ICAR ATRP, especially when the amount of catalyst decreases to the ppm level (*e.g.*, 6.3 ppm). All these primary results indicate that ICAR ATRP with AIBN, PMDETA and $BMPB_2$ is a controllable polymerization system.

Effect of catalyst concentration on polymerization of MMA

In ICAR ATRP, one of the advantages is that the dosage of catalyst is much lower than that of normal ATRP. In this work, the polymerizations were carried out with different amounts of organocopper catalyst (1.3–63.3 ppm). The results are shown in Table 3. It can be seen that when the catalyst concentrations are 1.9–3.3 ppm the $M_{n,GPC}$ values are close to the corresponding $M_{n,th}$ ones with narrow molecular weight distribution (M_w/M_n = 1.36–1.06), indicating well-controlled polymerizations; however if the catalyst concentration decreases to 1.3 ppm, the molecular weight distribution was relatively broad ($M_w/M_n = 1.51$).

To further understand the effect of catalyst concentration, the polymerization kinetics with different amounts of catalyst (1.3, 3.2, 6.3 ppm) were studied and the results are shown in Fig. 1. Fig. 1(a) shows the kinetic plots with molar ratios of $[MMA]_0 : [BMPB_2]_0 : [Cu(SC(S)N(C_4H_9)_2)_2]_0 : [PMDETA]_0 : [AIBN]_0 = 500 : 1 : x : 0.1 : 0.2$ (x = 0.001, 1.3 ppm Cu catalyst; 0.0025, 3.2 ppm; 0.005, 6.3 ppm). The time dependence of $\ln([M]_0/[M])$ is linear for various ratios of $Cu(SC(S)N(C_4H_9)_2)_2$ to AIBN, indicating that the number of the propagating radicals remains constant during the polymerization processes. From Fig. 1(a) it can be seen that there are induction periods (2.5–3.5 h), which are probably caused by impurities in the reaction system and the longer $t_{1/2}$ of AIBN (~10 h) at 65 °C. From Fig. 1(b), when the amounts of catalyst are 3.2 and 6.3 ppm, the molecular weights of PMMAs increase linearly with monomer conversion, and the molecular weight distributions remain low (M_w/M_n = 1.11–1.23). However, if the amount of catalyst is further decreased to 1.3 ppm, the molecular weights of the obtained PMMAs are larger than the corresponding theoretical ones; meanwhile the M_w/M_n values remain high (M_w/M_n = 1.32–1.55), indicating that the amount of catalyst should not be less than 1.3 ppm for a successful well-controlled polymerization process. These results indicated that the current ICAR ATRP with $Cu(SC(S)N(C_4H_9)_2)_2$ as the catalyst is a highly active system, even when the amount of catalyst is reduced to as low as 3.2 ppm.

Effect of AIBN concentration on polymerization of MMA

For a typical ICAR ATRP system, the thermal initiator such as AIBN plays a very important role, to continuously generate activators by an *in situ* reduction with the deactivators so as to make the dosage of catalyst very low, and the initial concentration of AIBN considerably influences the rate of polymerization. Fig. 2(a) shows the kinetic plots with different molar ratios of $[MMA]_0 : [BMPB_2]_0 : [Cu(SC(S)N\text{-}(C_4H_9)_2)_2]_0 : [PMDETA]_0 : [AIBN]_0 = 500 : 1 : 0.005 : 0.1 : x$ (x = 0.1, 0.2, 0.3, 0.5), which are approximately first order with respect to the monomer concentration, and the number of active species remains constant during these polymerization processes. It can be clearly observed that the rate of polymerization increases with an increasing amount of AIBN. For example, a monomer conversion of 65.0% can be obtained in 4.0 h at 65 °C for a

Table 1 Homogeneous ARGET/ICAR ATRP of MMA with 6.3 ppm of catalyst in the presence of different kinds of reducing agents (RAs)[a]

Entry	Molar ratio (R)	RA	Time (min)	Conv. (%)	$M_{n,th}$[b]	$M_{n,GPC}$	M_w/M_n
1	500 : 1 : 0.005 : 0.1 : 0.4	AsAc	200	65.3	32 600	36 200	1.68
2	500 : 1 : 0.005 : 0.1 : 0.2	$Sn(EH)_2$	520	48.9	24 500	27 200	1.24
3	500 : 1 : 0.005 : 0.1 : 0.2	AIBN	360	50.8	25 400	24 800	1.10

[a] Polymerization conditions: R = $[MMA]_0 : [BMPB_2]_0 : [Cu(SC(S)N(C_4H_9)_2)]_0 : [PMDETA]_0 : [RA]_0$, V_{MMA} = 3.0 mL, in bulk, temperature = 65 °C. [b] $M_{n,th} = ([M]_0/[BMPB_2]_0) \times M_{w,MMA} \times$ conversion %.

Downloaded by Soochow University China on 13/05/2013 12:53:07.
Published on 19 April 2013 on http://pubs.rsc.org | doi:10.1039/C3PY00309D

Table 2 Homogeneous ICAR ATRP of MMA with/without ligand or alkyl halide initiator[a]

Entry	Molar ratio (R)	Time (min)	Conv. (%)	$M_{n,th}$[b]	$M_{n,GPC}$	M_w/M_n
1	500 : 1 : 0.005 : 0.1 : 0.2	280	32.8	16 400	17 400	1.16
2	500 : 1 : 0.005 : 0 : 0.2	260	24.7	12 400	371 900	1.33
3	500 : 0 : 0.005 : 0.1 : 0.2	140	17.6	8800	259 300	1.67

[a] Polymerization conditions: R = $[MMA]_0 : [BMPB_2]_0 : [Cu(SC(S)N(C_4H_9)_2)_2]_0 : [PMDETA]_0 : [AIBN]_0$, V_{MMA} = 3.0 mL, in bulk, temperature = 65 °C. [b] $M_{n,th} = ([M]_0/[BMPB_2]_0) \times M_{w,MMA} \times$ conversion %.

molar ratio of $[AIBN]_0 : [Cu(SC(S)N(C_4H_9)_2)_2]_0$ = 0.5 : 0.005 (6.3 ppm Cu catalyst). This is attributed to the enhancement of catalyst regeneration ability with the increasing concentration of free radicals from AIBN decomposition, which act as the reducing agent to reduce Cu(II) species to active Cu(I) species. From Fig. 2(b), it can be seen that $M_{n,GPC}$ values increase linearly with monomer conversion and are close to their corresponding theoretical ones, while maintaining narrow M_w/M_n values (1.09–1.23).

Polymerization of MMA using $Cu(SeC(Se)N(C_4H_9)_2)_2$ as the catalyst

To further investigate the effect of the organocopper catalyst on ICAR ATRP, another organocopper catalyst, *N*,*N*-dibutyldiselenocarbamate copper ($Cu(SeC(Se)N(C_4H_9)_2)_2$), was synthesized in our lab to conduct the polymerization of MMA. Table 4 shows the bulk polymerization of MMA with different molar ratios $[MMA]_0 : [BMPB_2]_0 : [Cu(SeC(Se)N(C_4H_9)_2)_2]_0 : [PMDETA]_0 : [AIBN]_0$ = 500 : 1 : 0.0005–0.05 : 0.1 : 0.2 at 65 °C. As shown in Table 4, the $M_{n,GPC}$ values are close to the corresponding theoretical ones and the M_w/M_n values remain narrow (<1.40) until the catalyst concentration is decreased to 1.9 ppm.

Fig. 3(a) shows the kinetic plot of the bulk polymerization of MMA with the molar ratio $[MMA]_0 : [BMPB_2]_0 : [Cu(SeC(Se)N(C_4H_9)_2)_2]_0 : [PMDETA]_0 : [AIBN]_0$ = 500 : 1 : 0.005 (6.3 ppm) : 0.1 : 0.2 at 65 °C. It can be seen that the polymerization of MMA catalyzed by $Cu(SeC(Se)N(C_4H_9)_2)_2$ is approximately first order with respect to the monomer concentration, which indicates that the number of active species remains constant during the polymerization process. In addition, compared with the kinetic plot of $[Cu(SC(S)N(C_4H_9)_2)_2]_0 : [AIBN]_0$ = 0.005 : 0.2 in Fig. 1, by calculating the apparent rate constant of

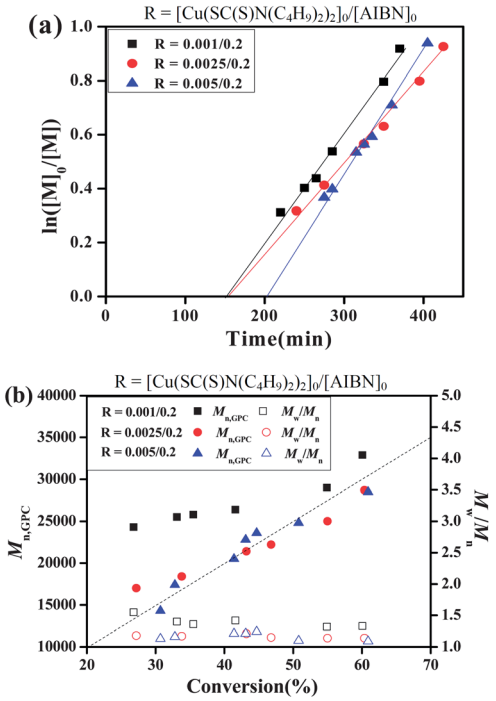

Fig. 1 $\ln([M]_0/[M])$ *versus* time (a) and number-average molecular weight ($M_{n,GPC}$) and molecular weight distribution (M_w/M_n) *versus* conversion (b) for the bulk ICAR ATRP of MMA with the molar ratio $[MMA]_0 : [BMPB_2]_0 : [Cu(SC(S)N(C_4H_9)_2)_2]_0 : [PMDETA]_0 : [AIBN]_0$ = 500 : 1 : *x* : 0.1 : 0.2 (*x* = 0.001, 1.3 ppm Cu catalyst; 0.0025, 3.2 ppm; 0.005, 6.3 ppm), V_{MMA} = 3.0 mL, temperature = 65 °C.

polymerization, k_p^{app} ($R_p = -d[M]/dt = k_p[P_n^{\cdot}][M] = k_p^{app}[M]$) as determined from the kinetic slopes, a k_p^{app} of 5.61×10^{-5} s^{-1} for the polymerization catalyzed by $Cu(SC(S)N(C_4H_9)_2)_2$ and a k_p^{app} of 5.66×10^{-5} s^{-1} for $Cu(SeC(Se)N(C_4H_9)_2)_2$ are obtained,

Table 3 Effect of the amount of catalyst on the homogeneous ICAR ATRP of MMA using $Cu(SC(S)N(C_4H_9)_2)_2$ as the catalyst[a]

Entry	Molar ratio (R)	Cu (ppm)	Conv. (%)	$M_{n,th}$[b]	$M_{n,GPC}$	M_w/M_n
1	500 : 1 : 0.001 : 0.1 : 0.2	1.3	47.1	23 600	34 000	1.51
2	500 : 1 : 0.0015 : 0.1 : 0.2	1.9	44.6	22 300	24 500	1.36
3	500 : 1 : 0.0025 : 0.1 : 0.2	3.2	41.8	20 900	19 900	1.17
4	500 : 1 : 0.0035 : 0.1 : 0.2	4.4	44.3	22 200	19 400	1.13
5	500 : 1 : 0.005 : 0.1 : 0.2	6.3	42.2	21 100	17 500	1.10
6	500 : 1 : 0.025 : 0.1 : 0.2	31.6	48.2	24 100	18 100	1.06
7	500 : 1 : 0.05 : 0.1 : 0.2	63.3	50.4	25 200	19 000	1.06

[a] Polymerization conditions: R = $[MMA]_0 : [BMPB_2]_0 : [Cu(SC(S)N(C_4H_9)_2)_2]_0 : [PMDETA]_0 : [AIBN]_0$, V_{MMA} = 3.0 mL, in bulk, polymerization time = 290 min, temperature = 65 °C. [b] $M_{n,th} = ([M]_0/[BMPB_2]_0) \times M_{w,MMA} \times$ conversion %.

This journal is © The Royal Society of Chemistry 2013

Downloaded by Soochow University China on 13/05/2013 12:53:07.
Published on 19 April 2013 on http://pubs.rsc.org | doi:10.1039/C3PY00309D

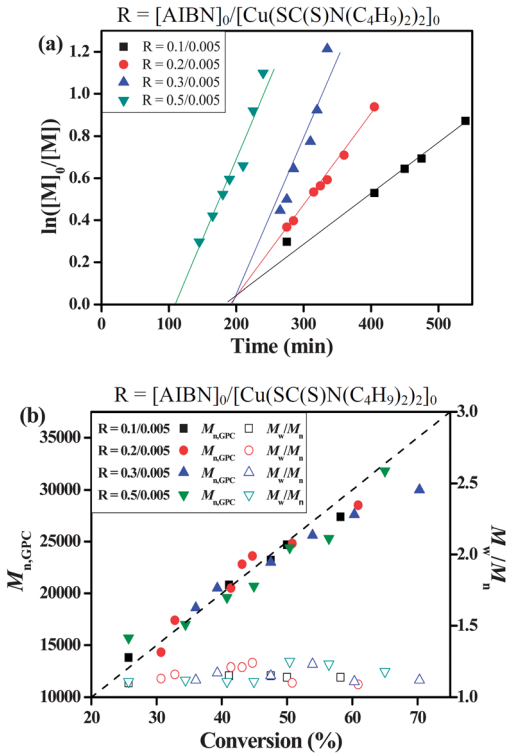

Fig. 2 ln([M]$_0$/[M]) *versus* time (a) and number-average molecular weight ($M_{n,GPC}$) and molecular weight distribution (M_w/M_n) *versus* conversion (b) for the bulk ICAR ATRP of MMA with the molar ratios [MMA]$_0$: [BMPB$_2$]$_0$: [Cu(SC(S)N(C$_4$H$_9$)$_2$)$_2$]$_0$: [PMDETA]$_0$: [AIBN]$_0$ = 500 : 1 : 0.005 : 0.1 : x (x = 0.1, 0.2, 0.3, 0.5), V_{MMA} = 3.0 mL, temperature = 65 °C.

Table 4 Effect of the amount of catalyst on the homogeneous ICAR ATRP of MMA using Cu(SeC(Se)N(C$_4$H$_9$)$_2$)$_2$ as the catalyst[a]

Entry	x	Cu (ppm)	Time (min)	Conv. (%)	$M_{n,th}$[b]	$M_{n,GPC}$	M_w/M_n
1	0.0005	0.6	295	45.5	22 800	41 900	1.84
2	0.001	1.3	340	49.5	24 800	33 900	1.71
3	0.0015	1.9	355	54.5	27 300	31 800	1.40
4	0.0025	3.2	390	58.7	29 400	30 300	1.25
5	0.0035	4.4	415	52.5	26 300	27 100	1.20
6	0.005	6.3	430	53.8	26 900	26 600	1.16
7	0.025	31.6	475	56.6	28 300	31 400	1.18
8	0.05	63.3	475	57.8	28 900	30 600	1.11

[a] Polymerization conditions: [MMA]$_0$: [BMPB$_2$]$_0$: [Cu(SeC(Se)N(C$_4$H$_9$)$_2$)$_2$]$_0$: [PMDETA]$_0$: [AIBN]$_0$ = 500 : 1 : x : 0.1 : 0.2 (x = 0.0005, 0.001, 0.0015, 0.0025, 0.0035, 0.005, 0.025, 0.05), V_{MMA} = 3.0 mL, in bulk, temperature = 65 °C. [b] $M_{n,th}$ = ([M]$_0$/[BMPB$_2$]$_0$) × $M_{w,MMA}$ × conversion %.

respectively. This means that the polymerization catalyzed by Cu(SeC(Se)N(C$_4$H$_9$)$_2$)$_2$ has almost the same polymerization rate as that catalyzed by Cu(SC(S)N(C$_4$H$_9$)$_2$)$_2$. Fig. 3(b) shows that the $M_{n,GPC}$ values increase linearly with monomer conversion and are close to their corresponding theoretical ones with narrow molecular weight distributions (M_w/M_n = 1.16–1.21), which are very similar to those catalyzed by Cu(SC(S)N(C$_4$H$_9$)$_2$)$_2$ with a molar ratio of [Cu(SC(S)N(C$_4$H$_9$)$_2$)$_2$]$_0$: [AIBN]$_0$ = 0.005 : 0.2 in

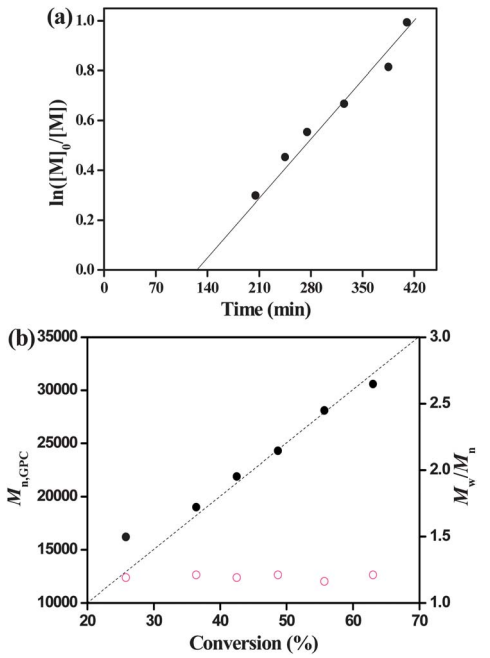

Fig. 3 ln([M]$_0$/[M]) *versus* time (a) and number-average molecular weight ($M_{n,GPC}$) and molecular weight distribution (M_w/M_n) *versus* conversion (b) for the bulk ICAR ATRP of MMA with the molar ratio [MMA]$_0$: [BMPB$_2$]$_0$: [Cu(SeC(Se)N(C$_4$H$_9$)$_2$)$_2$]$_0$: [PMDETA]$_0$: [AIBN]$_0$ = 500 : 1 : 0.005 : 0.1 : 0.2, V_{MMA} = 3.0 mL, temperature = 65 °C.

Fig. 1. These results indicate that Cu(SeC(Se)N(C$_4$H$_9$)$_2$)$_2$ can also be used as an efficient catalyst in this ICAR ATRP system, and the two catalysts Cu(SC(S)N(C$_4$H$_9$)$_2$)$_2$ and Cu(SeC(Se)N(C$_4$H$_9$)$_2$)$_2$ have similar catalytic activity.

In addition, in order to investigate whether a higher conversion can be obtained by this novel polymerization system, the polymerizations were carried out in the presence of 6.3 ppm and 63.3 ppm of catalyst. It can be seen from Fig. 4(a) that 85.3% and 87.3% monomer conversions can be obtained in 7.5 h when the amount of Cu(SC(S)N(C$_4$H$_9$)$_2$)$_2$ is 6.3 ppm and 63.3 ppm, respectively. However, a broader molecular weight distribution (M_w/M_n = 1.75) is obtained in the case of 6.3 ppm catalyst, in comparison with the value of M_w/M_n = 1.15 in the 63.3 ppm catalyst case, indicating that some side reactions may occur in the case of a very low concentration of catalyst if a higher conversion (more than 85%) is designed. A similar experimental phenomena was also observed when Cu(SeC(Se)N(C$_4$H$_9$)$_2$)$_2$ was used as the catalyst (Fig. 4(b)).

Analysis of chain end of PMMA using Cu(SC(S)N(C$_4$H$_9$)$_2$)$_2$ as the catalyst

The chain end of the PMMA was analyzed by ^{1}H NMR and UV-vis spectroscopy. Fig. 5 shows the ^{1}H NMR of PMMA produced using Cu(SC(S)N(C$_4$H$_9$)$_2$)$_2$ as the catalyst. The chemical shift at 7.05 ppm (a in Fig. 5) corresponds to the aromatic protons of the initiator BMPB$_2$. The chemical shift at 3.77 ppm (d in Fig. 5) is attributed to the methyl ester group at the chain end, which deviates from the chemical shift (3.60 ppm, e in Fig. 5) of the other methyl ester group in PMMA because of the

Downloaded by Soochow University China on 13/05/2013 12:53:07.
Published on 19 April 2013 on http://pubs.rsc.org | doi:10.1039/C3PY00309D

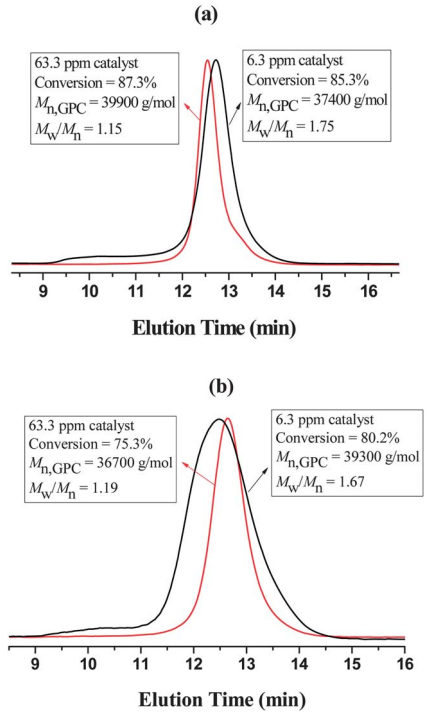

Fig. 4 GPC curves for the bulk ICAR ATRP of MMA in the presence of 6.3 ppm and 63.3 ppm catalyst, respectively. Polymerization conditions: (a) $[MMA]_0 : [BMPB_2]_0 : [Cu(SC(S)N(C_4H_9)_2)_2]_0 : [PMDETA]_0 : [AIBN]_0 = 500 : 1 : x : 0.1 : 0.2$, $V_{MMA} = 3.0$ mL, temperature = 65 °C, time = 7.5 h, conversion = 85.3% ($x = 0.005$, 6.3 ppm) and conversion = 87.3% ($x = 0.05$, 63.3 ppm); (b) $[MMA]_0 : [BMPB_2]_0 : [Cu(SeC(Se)N(C_4H_9)_2)_2]_0 : [PMDETA]_0 : [AIBN]_0 = 500 : 1 : x : 0.1 : 0.2$, $V_{MMA} = 3.0$ mL, temperature = 65 °C, conversion = 80.2% ($x = 0.005$, 6.3 ppm, time = 7.9 h) and conversion = 75.3% ($x = 0.05$, 63.3 ppm, time = 6.2 h).

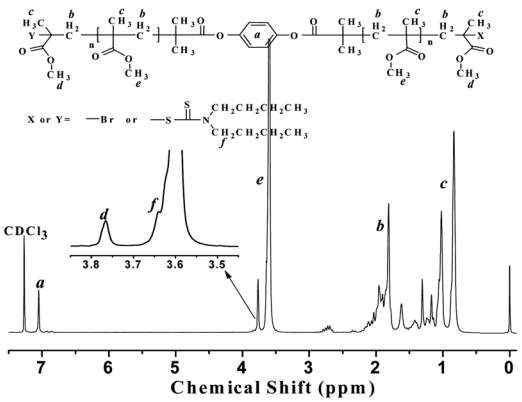

Fig. 5 ^{1}H NMR spectrum of PMMA ($M_{n,GPC} = 3000$ g mol^{-1}, $M_w/M_n = 1.11$) with $CDCl_3$ as solvent and tetramethylsilane (TMS) as an internal standard. Polymerization conditions: $[MMA]_0 : [BMPB_2]_0 : [Cu(SC(S)N(C_4H_9)_2)_2]_0 : [PMDETA]_0 : [AIBN]_0 = 500 : 1 : 0.05 : 0.1 : 0.2$, in bulk, $V_{MMA} = 3.0$ mL, temperature = 65 °C.

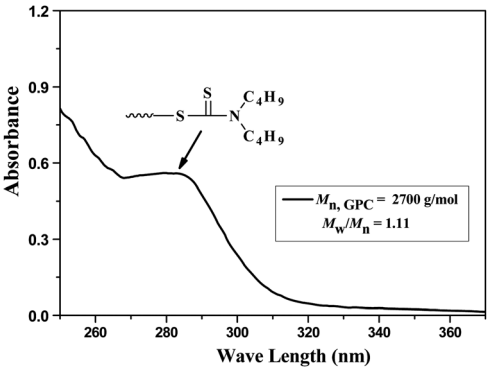

Fig. 6 UV-vis absorption of PMMA ($M_{n,GPC} = 2700$ g mol^{-1}, $M_w/M_n = 1.11$) in chloroform. Polymerization conditions: $[MMA]_0 : [BMPB_2]_0 : [Cu(SC(S)N(C_4H_9)_2)_2]_0 : [PMDETA]_0 : [AIBN]_0 = 500 : 1 : 0.05 : 0.1 : 0.2$, in bulk, $V_{MMA} = 3.0$ mL, temperature = 65 °C.

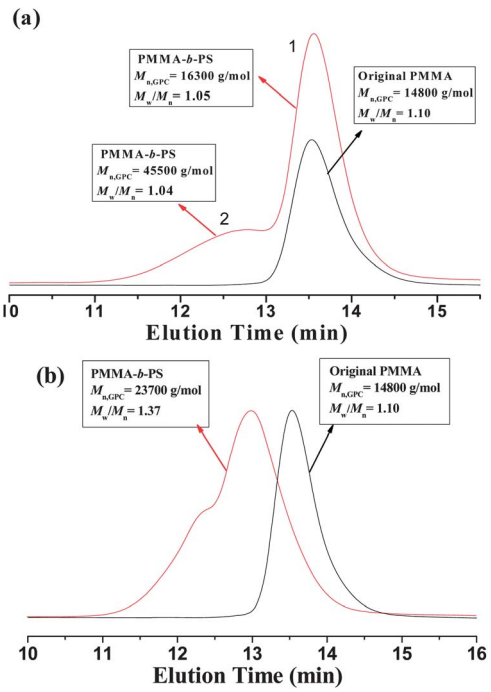

Fig. 7 (a) GPC curves before and after chain extension using PMMA as the macroinitiator *via* the iniferter mechanism. Polymerization conditions: $[St]_0 : [PMMA]_0 = 200 : 1$, $V_{St} = 0.5$ mL, $V_{toluene} = 1.0$ mL, time = 22 h, conversion = 18.6%, under 365 nm UV-vis light irradiation at room temperature. (b) GPC curves before and after chain extension using PMMA as the macroinitiator *via* the ATRP mechanism. Polymerization conditions: $[St]_0 : [PMMA]_0 : [CuBr]_0 : [PMDETA]_0 = 200 : 1 : 1 : 5$, $V_{St} = 0.5$ mL, $V_{toluene} = 1.0$ mL, temperature = 110 °C, time = 4 h, conversion = 18.9%. Original PMMA polymerization conditions: $[MMA]_0 : [BMPB_2]_0 : [Cu(SC(S)N(C_4H_9)_2)_2]_0 : [PMDETA]_0 : [AIBN]_0 = 500 : 1 : 0.05 : 0.1 : 0.2$, in bulk, $V_{MMA} = 3.0$ mL, temperature = 65 °C, time = 3.5 h, conversion = 31.4%.

electron-attracting function of the ω-Br[12] atom or the bibutylthiocarbamoythiyl group –S–C(=S)–N$(C_4H_9)_2$.[13] Furthermore, the integral value of peaks a to d was about 4 : 7, which is very close to the theoretical molar ratio of aromatic protons to methyl protons. The methylene protons of the end group $(–SC(S)N(CH_2CH_2CH_2CH_3)_2)_2$ (ref. 9, 14) at $\delta = 3.64$ ppm (f in Fig. 5) could also be observed. In addition, the UV-vis spectrum of the polymer is shown in Fig. 6; the absorption band due to –S–C(=S)–N$(C_4H_9)_2$ at 280 nm is consistent with previous reports,[15] which further confirms the presence of a –S–C(=S)–N$(C_4H_9)_2$ end-group in the obtained PMMA.

This journal is © The Royal Society of Chemistry 2013

Downloaded by Soochow University China on 13/05/2013 12:53:07.
Published on 19 April 2013 on http://pubs.rsc.org | doi:10.1039/C3PY00309D

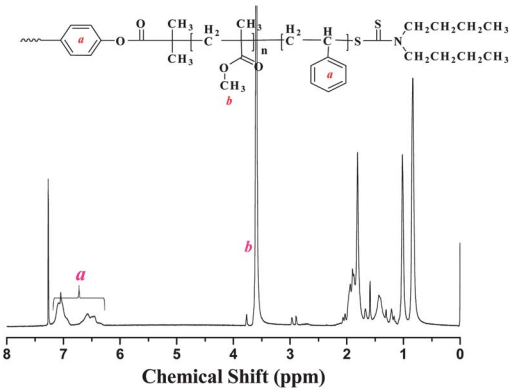

Fig. 8 ^{1}H NMR spectrum of PMMA-*b*-PS ($M_{n,GPC}$ = 16 300 g mol^{-1}, M_w/M_n = 1.05 and $M_{n,GPC}$ = 45 500 g mol^{-1}, M_w/M_n = 1.04) with $CDCl_3$ as the solvent and tetramethylsilane (TMS) as an internal standard. Polymerization conditions: $[St]_0$: $[PMMA]_0$ = 200 : 1, under 365 nm UV light irradiation at room temperature, V_{St} = 0.5 mL, $V_{toluene}$ = 1.0 mL, time = 22 h, conversion = 18.6%. The polymerization conditions of the macroinitiator PMMA ($M_{n,GPC}$ = 14 800 g mol^{-1}, M_w/M_n = 1.10): $[MMA]_0$: $[BMPB_2]_0$: $[Cu(SC(S)N(C_4H_9)_2)_2]_0$: $[PMDETA]_0$: $[AIBN]_0$ = 500 : 1 : 0.05 : 0.1 : 0.2, in bulk, V_{MMA} = 3.0 mL, temperature = 65 °C, time = 3.5 h, conversion = 31.4%.

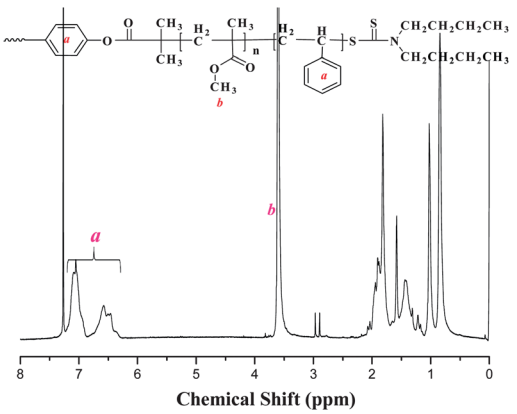

Fig. 9 ^{1}H NMR spectrum of PMMA-*b*-PS ($M_{n,GPC}$ = 23 700 g mol^{-1}, M_w/M_n = 1.37) with $CDCl_3$ as the solvent and tetramethylsilane (TMS) as an internal standard. Polymerization conditions: $[St]_0$: $[PMMA]_0$: $[CuBr]_0$: $[PMDETA]_0$ = 200 : 1 : 1 : 5, V_{St} = 0.5 mL, $V_{toluene}$ = 1.0 mL, temperature = 110 °C, time = 4 h, conversion = 18.9%. The polymerization conditions of the macroinitiator PMMA ($M_{n,GPC}$ = 14 800 g mol^{-1}, M_w/M_n = 1.10): $[MMA]_0$: $[BMPB_2]_0$: $[Cu(SC(S)N(C_4H_9)_2)_2]_0$: $[PMDETA]_0$: $[AIBN]_0$ = 500 : 1 : 0.05 : 0.1 : 0.2, in bulk, V_{MMA} = 3.0 mL, temperature = 65 °C, time = 3.5 h, conversion = 31.4%.

As we know, a polymer with a –S–C(=S)–N(C_4H_9)$_2$ end-group can act as a macroinitiator under UV-light irradiation *via* the iniferter mechanism. In order to further confirm this point, chain extension experiments were carried out *via* the iniferter mechanism. The chain extension experiments were carried out with styrene (St) as the fresh monomer under UV-light irradiation at room temperature. The GPC curves in Fig. 7(a) show only a few parts of the resultant PMMA with ω-S–C(=S)–N(C_4H_9)$_2$ in the chain end, which is verified by the peak shift from the original PMMA ($M_{n,GPC}$ = 14 800 g mol^{-1}, M_w/M_n = 1.10) to the chain-extended block copolymer PMMA-*b*-PS with $M_{n,GPC}$ = 45 500 g mol^{-1} and M_w/M_n = 1.04 (peak 2). This is due to the

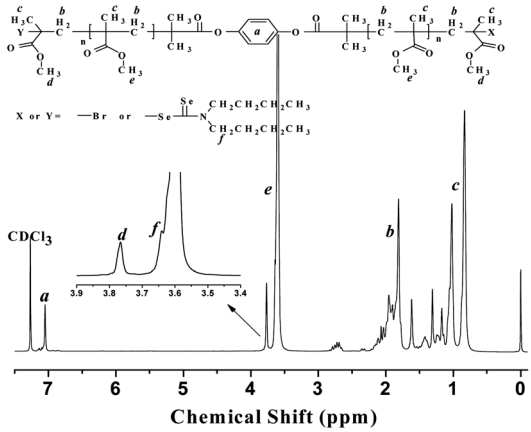

Fig. 10 ^{1}H NMR spectrum of PMMA ($M_{n,GPC}$ = 3200 g mol^{-1}, M_w/M_n = 1.11) with $CDCl_3$ as the solvent and tetramethylsilane (TMS) as an internal standard. Polymerization conditions: $[MMA]_0$: $[BMPB_2]_0$: $[Cu(SeC(Se)N(C_4H_9)_2)_2]_0$: $[PMDETA]_0$: $[AIBN]_0$ = 500 : 1 : 0.05 : 0.1 : 0.2, in bulk, V_{MMA} = 3.0 mL, temperature = 65 °C.

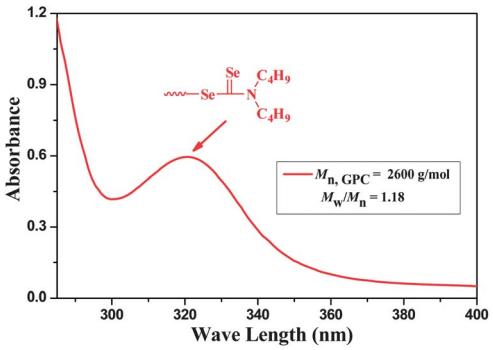

Fig. 11 UV-vis absorption of PMMA ($M_{n,GPC}$ = 2600 g mol^{-1}, M_w/M_n = 1.18) in chloroform. Polymerization conditions: $[MMA]_0$: $[BMPB_2]_0$: $[Cu(SeC(Se)N(C_4H_9)_2)_2]_0$: $[PMDETA]_0$: $[AIBN]_0$ = 500 : 1 : 0.05 : 0.1 : 0.2, in bulk, V_{MMA} = 3.0 mL, temperature = 65 °C.

fact that large parts of the as-prepared PMMAs ($M_{n,GPC}$ = 16 300 g mol^{-1} and M_w/M_n = 1.05) cannot initiate chain extension polymerization *via* the iniferter mechanism under UV irradiation due to the presence of ω-Br in the chain ends of the macroinitiators.

In order to confirm the existence of ω-Br in the chain ends of PMMAs, the chain extension experiment at 110 °C was carried out with St as the fresh monomer and CuBr/PMDETA as the catalyst *via* a typical ATRP mechanism. Fig. 7(b) shows that the molecular weight increases from 14 800 g mol^{-1} to 23 700 g mol^{-1} after chain extension, which proves that most of PMMA chains are "living" (with ω-Br or ω-S–C(=S)–N(C_4H_9)$_2$ end groups), although the M_w/M_n value becomes larger and a shoulder peak exists in GPC curves. The broad peak with a shoulder is probably due to the different activities of the end groups of ω-Br and ω-S–C(=S)–N(C_4H_9)$_2$ and a minority of unavoidable dead chains among the macroinitiators formed by biradical termination during the ICAR ATRP process.

In addition, the resultant block copolymer PMMA-*b*-PS was further confirmed by ^{1}H NMR spectra, as shown in Fig. 8 and 9.

Downloaded by Soochow University China on 13/05/2013 12:53:07.
Published on 19 April 2013 on http://pubs.rsc.org | doi:10.1039/C3PY00309D

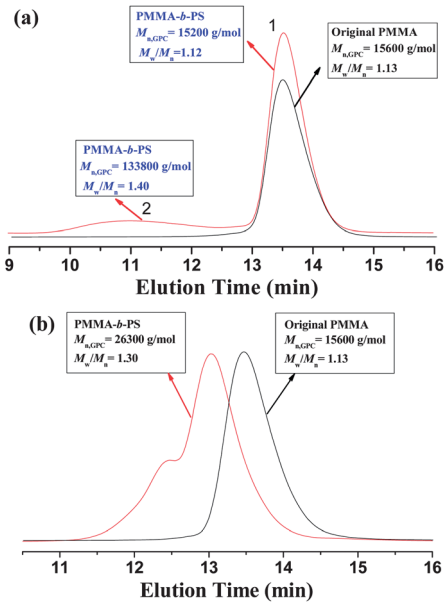

Fig. 12 (a) GPC curves before and after chain extension using PMMA as the macroinitiator *via* the iniferter mechanism. Polymerization conditions: $[St]_0 : [PMMA]_0 = 200 : 1$, $V_{St} = 0.5$ mL, $V_{toluene} = 1.0$ mL, time = 30 h, conversion = 7.2%, under 365 nm UV-vis light irradiation at room temperature. (b) GPC curves before and after chain extension using PMMA as the macroinitiator *via* the ATRP mechanism. Polymerization conditions: $[St]_0 : [PMMA]_0 : [CuBr]_0 : [PMDETA]_0 = 200 : 1 : 1 : 5$, $V_{St} = 0.5$ mL, $V_{toluene} = 1.0$ mL, temperature = 110 °C, time = 4 h, conversion = 16.4%. Original PMMA polymerization conditions: $[MMA]_0 : [BMPB_2]_0 : [Cu(SeC(Se)N(C_4H_9)_2)_2]_0 : [PMDETA]_0 : [AIBN]_0 = 500 : 1 : 0.05 : 0.1 : 0.2$, in bulk, $V_{MMA} = 3.0$ mL, temperature = 65 °C, time = 3.5 h, conversion = 34.8%.

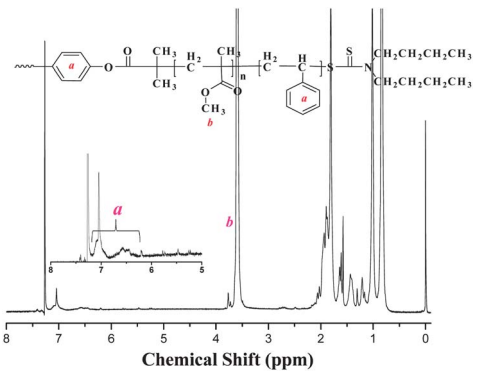

Fig. 13 ^{1}H NMR spectrum of PMMA-*b*-PS ($M_{n,GPC}$ = 15 200 g mol^{-1}, M_w/M_n = 1.12 and $M_{n,GPC}$ = 133 800 g mol^{-1}, M_w/M_n = 1.40) with $CDCl_3$ as the solvent and tetramethylsilane (TMS) as an internal standard. Polymerization conditions: $[St]_0 : [PMMA]_0 = 200 : 1$, under 365 nm UV light irradiation at room temperature, V_{St} = 0.5 mL, $V_{toluene}$ = 1.0 mL, time = 30 h, conversion = 7.2%. The polymerization conditions of the macroinitiator PMMA ($M_{n,GPC}$ = 15 600 g mol^{-1}, M_w/M_n = 1.13): $[MMA]_0 : [BMPB_2]_0 : [Cu(SeC(Se)N(C_4H_9)_2)_2]_0 : [PMDETA]_0 : [AIBN]_0 = 500 : 1 : 0.05 : 0.1 : 0.2$, in bulk, V_{MMA} = 3.0 mL, temperature = 65 °C, time = 3.5 h, conversion = 34.8%.

The chemical shifts at $\delta = 6.37$–7.08 ppm (a in Fig. 8 and 9) for the aromatic protons of PS and at $\delta = 3.60$ ppm (b in Fig. 8 and 9) for the protons of the methyl ester group in PMMA chains indicate the successful block copolymerization.

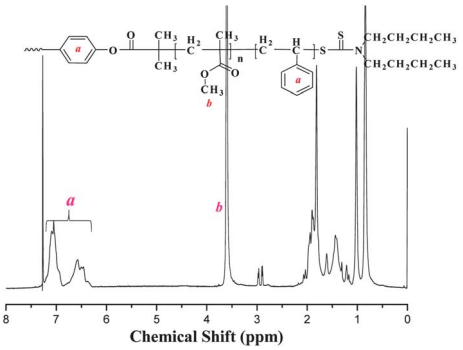

Fig. 14 ^{1}H NMR spectrum of PMMA-*b*-PS ($M_{n,GPC}$ = 26 300 g mol^{-1}, M_w/M_n = 1.30) with $CDCl_3$ as the solvent and tetramethylsilane (TMS) as an internal standard. Polymerization conditions: $[St]_0 : [PMMA]_0 : [CuBr]_0 : [PMDETA]_0 = 200 : 1 : 1 : 5$, V_{St} = 0.5 mL, $V_{toluene}$ = 1.0 mL, temperature = 110 °C, time = 4 h, conversion = 16.4%. The polymerization conditions of the macroinitiator PMMA ($M_{n,GPC}$ = 15 600 g mol^{-1}, M_w/M_n = 1.13): $[MMA]_0 : [BMPB_2]_0 : [Cu(SeC(Se)N(C_4H_9)_2)_2]_0 : [PMDETA]_0 : [AIBN]_0 = 500 : 1 : 0.05 : 0.1 : 0.2$, in bulk, V_{MMA} = 3.0 mL, temperature = 65 °C, time = 3.5 h, conversion = 34.8%.

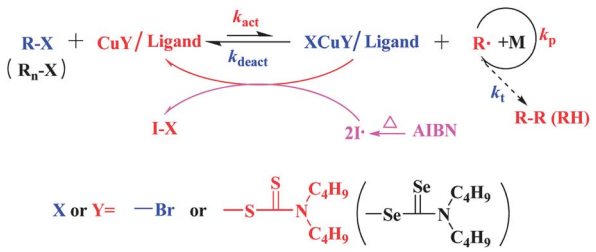

Scheme 1 Plausible mechanism for the organocopper-mediated ICAR ATRP.

Analysis of chain end of PMMA using $Cu(SeC(Se)N(C_4H_9)_2)_2$ as the catalyst

Similarly, when using $Cu(SeC(Se)N(C_4H_9)_2)_2$ instead of $Cu(SC(S)N(C_4H_9)_2)_2$ as the catalyst, the chemical shifts at $\delta = 7.05$ ppm (a in Fig. 10), 3.77 ppm (d in Fig. 10) and 3.64 ppm (f in Fig. 10) in combination with the UV-vis absorption band at 325 nm due to –Se–C(=Se)–$N(C_4H_9)_2$ (ref. 11c) (Fig. 11) indicate the successful attachment of ω-Br and ω-Se–C(=Se)–$N(C_4H_9)_2$ onto the chain end of the resultant PMMAs.

In addition, the chain extension experiments were also carried out with St as the fresh monomer *via* the iniferter mechanism under UV-light irradiation at room temperature and *via* the ATRP mechanism at 110 °C. In Fig. 12(a), the peak shifts from the macroinitiator ($M_{n,GPC} = 15\,600$ g mol^{-1}, $M_w/M_n = 1.13$) to the block copolymer PMMA-*b*-PS with $M_{n,GPC}$ = 133 800 g mol^{-1} and M_w/M_n = 1.40 (peak 2) *via* the iniferter method; Fig. 12(b) shows a peak shift from that with $M_{n,GPC}$ = 15 600 g mol^{-1} to that with $M_{n,GPC} = 26\,300$ g mol^{-1} after chain extension *via* ATRP of St. Fig. 13 and 14 show ^{1}H NMR spectra of the obtained block copolymer PMMA-*b*-PS. The chemical shifts at $\delta = 6.37$–7.08 ppm (a in Fig. 13 and 14) for the aromatic protons of PS and at $\delta = 3.60$ ppm (b in Fig. 13 and 14) for the protons of the methyl ester group in the PMMA chains indicate the successful block copolymerization. As discussed above, all these results confirm that almost all of the chain ends of the PMMAs

This journal is © The Royal Society of Chemistry 2013

Published on 19 April 2013 on http://pubs.rsc.org | doi:10.1039/C3PY00309D
Downloaded by Soochow University China on 13/05/2013 12:53:07.

synthesized using $Cu(SeC(Se)N(C_4H_9)_2)_2$ as the catalyst have ω-Br or ω-Se–C(=Se)–$N(C_4H_9)_2$ groups attached.

Plausible mechanism of organocopper-catalyzed polymerization

As discussed above, it can be concluded that the organocopper-mediated ICAR ATRP mechanism is similar to that reported previously.[5,7] Herein, as shown in Scheme 1, I˙ free radicals are slowly and continuously generated by the conventional radical initiator AIBN throughout the polymerization, to constantly reduce the Cu(II) complex that accumulates as a persistent radical to a Cu(I) complex. Then the propagating radical R˙ can be regenerated by the reversible redox reaction between the Cu(I) complex and the ATRP initiator R–X as proceeded by the normal ATRP mechanism. However, due to the exchange of chain ends between ω-Br and DC groups (ω-S–C(=S)–$N(C_4H_9)_2$ or ω-Se–C(=Se)–$N(C_4H_9)_2$), some end chains were ended by DC groups.

Conclusion

A highly active homogeneous ICAR ATRP system was successfully developed using $Cu(SC(S)N(C_4H_9)_2)_2$ or $Cu(SeC(Se)N(C_4H_9)_2)_2$ as the organocatalyst and MMA as the model monomer. The amount of catalyst can be decreased to less than 2 ppm levels while maintaining the typical "living" features of ATRP, such as tunable molecular weights and low molecular weight distributions for the resultant PMMAs.

Acknowledgements

Financial support from the National Natural Science Foundation of China (no. 21174096, 21274100 and 21234005), the Specialized Research Fund for the Doctoral Program of Higher Education (no. 20103201110005), the Project of International Cooperation of the Ministry of Science and Technology of China (no. 2011DFA50530), and the Project Funded by the Priority Academic Program Development of Jiangsu Higher Education Institutions (PAPD) is gratefully acknowledged.

Notes and references

1 (*a*) V. Coessens, T. Pintauer and K. Matyjaszewski, *Prog. Polym. Sci.*, 2001, **26**, 337; (*b*) K. Matyjaszewski, *Prog. Polym. Sci.*, 2005, **30**, 858; (*c*) H. B. Dong, Y. Y. Xu and Z. Yi, *Chin. J. Polym. Sci.*, 2009, **27**, 813; (*d*) M. Ouchi, T. Terashima and M. Sawamoto, *Chem. Rev.*, 2009, **109**, 4963; (*e*) Q. Li, L. F. Zhang, Z. B. Zhang, N. C. Zhou, Z. P. Cheng and X. L. Zhu, *J. Polym. Sci., Part A: Polym. Chem.*, 2010, **48**, 2006; (*f*) W. D. Liu, Y. H. Zhang, L. F. Fang, B. K. Zhu and L. P. Zhu, *Chin. J. Polym. Sci.*, 2012, **30**, 568; (*g*) Y. P. Borguet and N. V. Tsarevsky, *Polym. Chem.*, 2012, **3**, 2487; (*h*) X. X. Chen, M. Y. Khan and S. K. Noh, *Polym. Chem.*, 2012, **3**, 1971; (*i*) W. W. Li and K. Matyjaszewski, *Polym. Chem.*, 2012, **3**, 1813; (*j*) F. J. Xu, K. G. Neoh and E. T. Kang, *Prog. Polym. Sci.*, 2009, **34**, 719; (*k*) L. J. Bai, L. F. Zhang, Z. P. Cheng and X. L. Zhu, *Polym. Chem.*, 2012, **3**, 2685; (*l*) T. Guo, L. F. Zhang, H. J. Jiang, Z. B. Zhang, J. Zhu, Z. P. Cheng and X. L. Zhu, *Polym. Chem.*, 2011, **2**, 2385.

2 (*a*) M. Kato, M. Kamigaito, M. Sawamoto and T. Higashimura, *Macromolecules*, 1995, **28**, 1721; (*b*) K. Matyjaszewski, W. Jakubowski, K. Min, W. Tang, J. Huang, W. A. Braunecker and N. V. Tsarevsky, *Proc. Natl. Acad. Sci. U. S. A.*, 2006, **103**, 15309.

3 (*a*) L. Mueller and K. Matyjaszewski, *Macromol. React. Eng.*, 2010, **4**, 180; (*b*) K. Matyjaszewski, T. Pintauer and S. Gaynor, *Macromolecules*, 2000, **33**, 1476; (*c*) Y. Shen, H. Tang and S. Ding, *Prog. Polym. Sci.*, 2004, **29**, 1053; (*d*) S. Ding, M. Radosz and Y. Shen, *Macromolecules*, 2005, **38**, 5921; (*e*) S. Faucher and S. Zhu, *J. Polym. Sci., Part A: Polym. Chem.*, 2007, **45**, 553; (*f*) N. V. Tsarevsky and K. Matyjaszewski, *Chem. Rev.*, 2007, **107**, 2270.

4 (*a*) N. Chan, M. F. Cunningham and R. A. Hutchinson, *Macromol. React. Eng.*, 2010, **4**, 369; (*b*) N. Chan, M. F. Cunningham and R. A. Hutchinson, *Macromol. Chem. Phys.*, 2008, **209**, 1797; (*c*) W. Jakubowski and K. Matyjaszewski, *Angew. Chem., Int. Ed.*, 2006, **45**, 4482; (*d*) W. Jakubowski, K. Min and K. Matyjaszewski, *Macromolecules*, 2006, **39**, 39; (*e*) Y. Wang, Y. Z. Zhang, B. Parker and K. Matyjaszewski, *Macromolecules*, 2011, **44**, 4022.

5 (*a*) G. H. Zhu, L. F. Zhang, Z. B. Zhang, J. Zhu, Y. F. Tu, Z. P. Cheng and X. L. Zhu, *Macromolecules*, 2011, **44**, 3233; (*b*) K. Mukumoto, Y. Wang and K. Matyjaszewski, *ACS Macro Lett.*, 2012, **1**, 599; (*c*) D. Konkolewicz, A. J. D. Magenau, S. E. Averick, A. Simakova, H. He and K. Matyjaszewski, *Macromolecules*, 2012, **45**, 4461; (*d*) G. Wang, M. Lu and Y. Liu, *J. Appl. Polym. Sci.*, 2012, **126**, 381; (*e*) X. Liu, J. Wang, F. Zhang, S. An, Y. Ren, Y. Yu, P. Chen and S. Xie, *J. Polym. Sci., Part A: Polym. Chem.*, 2012, **50**, 4358; (*f*) G. Wang, M. Lu and H. Wu, *Polymer*, 2012, **53**, 1093; (*g*) X. Liu, J. Wang, J. Yang, S. An, Y. Ren, Y. Yu and P. Chen, *J. Polym. Sci., Part A: Polym. Chem.*, 2012, **50**, 1933.

6 (*a*) A. J. D. Magenau, N. C. Strandwitz, A. Gennaro and K. Matyjaszewski, *Science*, 2011, **332**, 81; (*b*) N. Bortolamei, A. A. Isse, A. J. D. Magenau, A. Gennaro and K. Matyjaszewski, *Angew. Chem., Int. Ed.*, 2011, **123**, 11593.

7 (*a*) A. Plichta, W. Li and K. Matyjaszewski, *Macromolecules*, 2009, **42**, 2330; (*b*) T. Pintauer and K. Matyjaszewski, *Chem. Soc. Rev.*, 2008, **37**, 1087; (*c*) W. A. Braunecker and K. Matyjaszewski, *Prog. Polym. Sci.*, 2007, **32**, 93; (*d*) L. F. Zhang, J. Miao, Z. P. Cheng and X. L. Zhu, *Macromol. Rapid Commun.*, 2010, **31**, 275.

8 (*a*) V. Percec, A. Asandei, F. Asgarzadeh, B. Barboiu, M. Holerca and C. Grigoras, *J. Polym. Sci., Part A: Polym. Chem.*, 2000, **38**, 4353; (*b*) D. Qin, S. Qin and K. Qiu, *J. Polym. Sci., Part A: Polym. Chem.*, 2001, **39**, 3464; (*c*) P. Li and K. Qiu, *Macromol. Rapid Commun.*, 2002, **23**, 1124; (*d*) K. Y. Qiu and P. Li, *Chin. J. Polym. Sci.*, 2004, **22**, 99; (*e*) P. Li and K. Qiu, *Macromolecules*, 2002, **35**, 8906; (*f*) W. Zhang, X. L. Zhu, J. Zhu and Z. P. Cheng, *Macromol.*

Chem. Phys., 2004, **205**, 806; (*g*) S. H. Qin, D. Q. Qin and K. Y. Qiu, *Chin. J. Polym. Sci.*, 2001, **19**, 441.

9 (*a*) M. Bonamico, G. Dessy, A. Mugnoli, A. Vaciago and L. Zambonelli, *Acta Crystallogr.*, 1965, **19**, 886; (*b*) G. Newton, H. D. Caughman and R. C. Taylor, *J. Chem. Soc., Dalton Trans.*, 1974, 258; (*c*) Y. Kwak and K. Matyjaszewski, *Macromolecules*, 2008, **41**, 6627; (*d*) P. Li and K. Y. Qiu, *Macromol. Chem. Phys.*, 2002, **203**, 2305; (*e*) P. Li and K. Y. Qiu, *J. Polym. Sci., Part A: Polym. Chem.*, 2002, **40**, 2093.

10 (*a*) J. Rotruck, A. Pope, H. Ganther, A. Swanson, D. Hafeman and W. Hoekstra, *Science*, 1973, **179**, 588; (*b*) H. Xu, J. Gao, Y. Wang, Z. Wang, M. Dehaen and X. Zhang, *Chem. Commun.*, 2006, 796; (*c*) X. Zhang, H. Xu, Z. Dong, Y. Wang, J. Liu and J. Shen, *J. Am. Chem. Soc.*, 2004, **126**, 10556.

11 (*a*) D. Barnard and D. Woodbridge, *J. Chem. Soc.*, 1961, 2922; (*b*) D. M. Haddleton and C. Waterson, *Macromolecules*, 1999, **32**, 8732; (*c*) K. Jensen and V. Krishnan, *Acta Chem. Scand.*, 1970, **24**, 2055.

12 L. F. Zhang, Z. P. Cheng, F. Tang, Q. Li and X. L. Zhu, *Macromol. Chem. Phys.*, 2008, **209**, 1705.

13 G. H. Zhu, L. F. Zhang, X. Q. Pan, W. Zhang, Z. P. Cheng and X. L. Zhu, *Macromol. Rapid Commun.*, 2012, **33**, 2121.

14 G. Eng, X. Song, Q. Duong, D. Strickman, J. Glass and L. May, *Appl. Organomet. Chem.*, 2003, **17**, 218.

15 T. Otsu and M. Yoshida, *Polym. Bull.*, 1982, **7**, 197.

Downloaded by Soochow University China on 13/05/2013 12:53:07.
Published on 19 April 2013 on http://pubs.rsc.org | doi:10.1039/C3PY00309D

 This journal is © The Royal Society of Chemistry 2013